Discovery of Potent, Highly Selective, and Orally Bioavailable Pyridine Carboxamide c-Jun NH_2-Terminal Kinase Inhibitors

Hongyu Zhao,* Michael D. Serby, Zhili Xin, Bruce G. Szczepankiewicz, Mei Liu, Christi Kosogof, Bo Liu, Lissa T. J. Nelson, Eric F. Johnson, Sanyi Wang, Terry Pederson, Rebecca J. Gum, Jill E. Clampit, Deanna L. Haasch, Cele Abad-Zapatero, Elizabeth H. Fry, Cristina Rondinone, James M. Trevillyan, Hing L. Sham, and Gang Liu

Metabolic Disease Research, Global Pharmaceutical Research and Development, Abbott Laboratories, 100 Abbott Park Road, Abbott Park, Illinois 60064-6098

Received April 19, 2006

Abstract: C-Jun NH_2 terminal kinases (JNKs) are important cell signaling enzymes. JNK1 plays a central role in linking obesity and insulin resistance. JNK2 and JNK3 may be involved in inflammatory and neurological disorders, respectively. Small-molecule JNK inhibitors could be valuable tools to study the therapeutic benefits of inhibiting these enzymes and as leads for potential drugs targeting JNKs. In this report, we disclose a series of potent and highly selective JNK inhibitors with good pharmacokinetic profiles.

JNKs[a] are members of a family of important signal transducing enzymes known as mitogen-activated protein kinases and can be activated by a variety of stress factors.[1] Three distinct genes (encoded JNK1, JNK2, and JNK3, respectively) have been identified,[2] and their up-regulation has been associated with several disorders. JNK2 plays an important role in autoimmune and inflammatory diseases,[3] while JNK3 might be involved in neurological disorders.[4] We were particularly interested in JNK1, a key enzyme linking insulin resistance and obesity. Obesity is associated with low-level inflammation[5] and is closely related to diabetes. Adipose tissue, now recognized as an important endocrine organ, secretes a number of hormones that lead to insulin resistance.[6] Among these hormones, inflammatory cytokines and free fatty acids were found to activate JNKs.[7] Upon activation, JNK1 phosphorylates IRS1 at Ser^{307} (rat IRS1, Ser^{312} for human IRS1)[8] and inhibits the interaction between IRS1 and insulin receptor,[9] providing a putative mechanism to explain the insulin resistance that occurs in inflammatory and obese states. Absence of the JNK1 gene protects mice from diet-induced obesity and obesity-induced insulin resistance and results in decreased adiposity and enhanced secretion of the adiponectin.[10] Genetically obese mice (ob/ob) with targeted disruption of the JNK1 gene (ob/ob JNK1−/−) are leaner and maintain lower blood glucose and insulin levels compared with ob/ob JNK1+/+ mice.[10] Administration of a JNK-inhibitory cell-permeable JIP1 derivative for 14 days greatly improved insulin sensitivity and glucose tolerance in diabetic db/db mice.[11] A small-molecule JNK1 inhibitor of undisclosed identity was reported to improve fasting glucose levels and glucose tolerance in db/db mice.[12] A number of JNK inhibitors have been reported in recent years.[13] Here, we report a novel series of potent, selective, and orally bioavailable JNK inhibitors. These inhibitors could be useful research tools for studying the crucial role of JNKs in cell signaling to evaluate their validity as therapeutic targets. They are also good leads for potential drugs targeting JNKs.

Screening of Abbott Laboratories' compound collection identified acylaminopyridine derivative **1** as a JNK1 inhibitor (Figure 1). This compound was synthesized by reacting malononitrile with HBr[14] followed by displacement of the bromo group with an ethoxy group[15] and selective acetylation of the 2-amino group of the resulting aminopyridine. A number of 2-acylaminopyridines analogous to **1** have been synthesized and screened, and phenylacetylamides were proved to be optimal (e.g., **2** showed an IC_{50} of 45 nM, Figure 1).[16] However, these analogues generally suffered from poor metabolic stability and oral bioavailability. The throughput of producing 2-acylaminopyridine analogues was low because the inert 2-amino group only reacts with acid chlorides. This synthetic sequence also limited the SAR exploration of other positions of the pyridine core in **1**. To overcome the synthetic accessibility and the metabolic stability hurdles, 2-pyridinecarboxamide analogues such as **3** were synthesized ("reversed" amides, Figure 1). Inhibitors **3** and **2** were nearly equipotent, suggesting that the "reversed" amide scaffold was comparable to the "normal" amide counterpart in binding efficiency. The amide bond in **3** was formed by a standard TBTU mediated amide formation reaction. This reaction allowed a large number of amides to be synthesized and screened quickly. Also, the pyridine core was assembled in a more controlled, stepwise manner so that all positions on the pyridine ring could be systematically studied. Analogues based on this new scaffold consistently demonstrated much improved PK profiles.

The synthesis of **3**, **6**, and **8a**−**g** (Scheme 1) began with the known hydroxypyridine **4**.[17] Transforming the hydroxy group in **4** to a triflate group (intermediate **5**) followed by a palladium mediated carbonylation reaction[18] and a saponification reaction yielded carboxylic acid **7**. A TBTU mediated amide coupling between **7** and the corresponding commercially available amines produced **3**, **8a**−**e**, and **8g**. For the synthesis of inhibitor **8f**, acid **7** was first coupled to 5-aminomethyl-2-chloropyridine via a TBTU coupling reaction and the resulting chloropyridine amide was coupled to 4-methoxycarbonylphenylboronic acid via a Suzuki type coupling reaction. Saponification of the ester in the Suzuki coupling product provided **8f**. Displacement of the triflate group in **5** with 2,5-dimethoxybenzylamine gave **6**.

The synthesis of **12**, **13**, **15**, **17a**, and **17b** is outlined in Scheme 2. Selective chlorination of the 5-position of the known picolinic acid ester **9**[16] followed by saponification of the ester provided acid **10**. The ethoxy group in **10** was cleaved in 6 N aqueous HCl solution,[19] and the resulting hydroxy acid was treated with 2 equiv of 2-iodopropane and Ag_2CO_3[20] followed by saponification of the resulting ester to yield acid **11**. Amides **12** and **13** were obtained by a TBTU mediated amide coupling reaction as described above. Amides **15**, **17a**, and **17b** were made using a similar reaction sequence that transformed **4** to **8** (see Scheme 1) starting from the known hydroxypyridines **14**[21] and **16**,[17] respectively.

The SAR results are summarized in Table 1. The ATP binding sites among JNKs are highly conserved, which presents a great challenge for developing isoform selective inhibitors. The

* To whom correspondence should be addressed. Phone: 847-935-4566. Fax: 847-938-1674. E-mail: Hongyu.zhao@abbott.com.

[a] Abbreviations: JNK, c-Jun NH_2 terminal kinase; MAPKs, mitogen-activated protein kinases; IRS1, insulin receptor substrate 1; JIP1, JNK-interacting protein-1; TBTU, 2-(1*H*-benzotriazole-1-yl)-1,1,3,3-tetramethyluronium tetrafluoroborate; PK, pharmacokinetic; AUC, area under the curve.

10.1021/jm060465l CCC: $33.50
Published on Web 06/30/2006

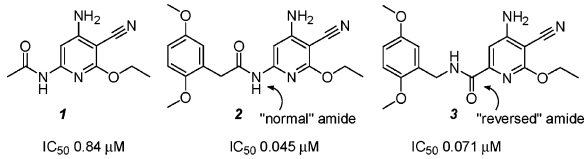

Figure 1. 2-Acylaminopyridine and 2-pyridinecarboxamide JNK inhibitors.

Scheme 1. Synthesis of Inhibitors **3**, **6**, **8a**−**g**[a]

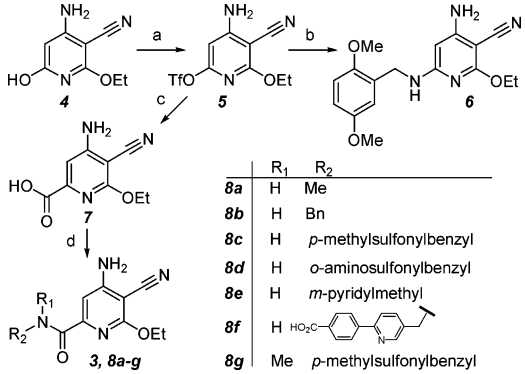

[a] Reagents and conditions: (a) Tf_2NPh, Et_3N, room temp (60%); (b) 2,5-dimethoxybenzylamine, DMSO, 110 °C, 73%; (c) (1) CO, $PdCl_2(dppf)$-CH_2Cl_2, MeOH, 50 °C, 50%; (2) LiOH, MeOH−H_2O, room temp, 76%. (d) For **3**, **8a**−**e**,**g**: corresponding commercially available amines, TBTU, Et_3N, DMF, room temp. For **8f**: (1) 5-aminomethyl-2-chloropyridine, TBTU, Et_3N, DMF, room temp; (2) 4-methoxycarbonylphenylboronic acid, $Pd(Ph_3P)_4$, aqueous K_2CO_3, toluene, 49%; (3) LiOH, MeOH−H_2O, room temp, 59%.

Scheme 2. Synthesis of Inhibitors **12**, **13**, **15**, **17a**, and **17b**[a]

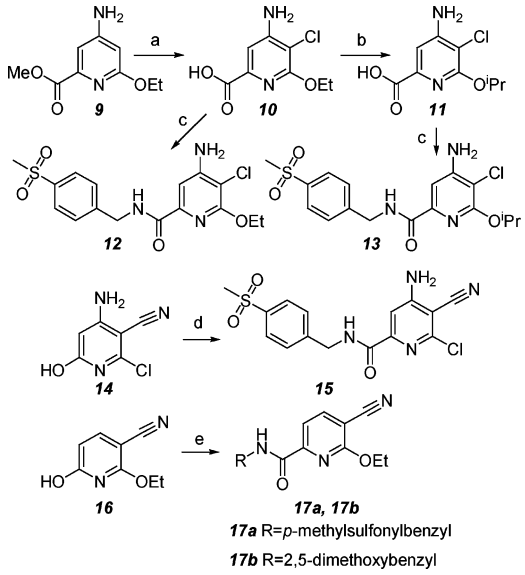

[a] Reagents and conditions: (a) (1) *N*-chlorosuccinimide, DMF, room temp, 48%; (2) LiOH, MeOH−H_2O, room temp, 70%; (b) (1) 6 N aqueous HCl, 145 °C, 84%; (2) *i*-PrI, Ag_2CO_3, 100 °C, 37%; (3) LiOH, MeOH−H_2O, room temp, 100%; (c) *p*-methylsulfonylbenzylamine, TBTU, Et_3N, DMF, room temp; (d) (1) Tf_2O, Et_3N, room temp, 69%; (2) CO, $PdCl_2(dppf)CH_2Cl_2$, MeOH, room temp, 72%; (3) NaOH, MeOH−H_2O, room temp, 82%; (4) *p*-methylsulfonylbenzylamine, TBTU, Et_3N, DMF, room temp, 88%; (e) (1) Tf_2NPh, Et_3N, room temp, 69%; (2) CO, $PdCl_2(dppf)CH_2Cl_2$, MeOH, 50 °C, 32% over two steps; (3) LiOH, MeOH−H_2O, room temp, 71%; (4) corresponding benzylamines, TBTU, Et_3N, DMF, room temp, 39% for **17a**, 42% for **17b**.

selectivity among JNKs of the inhibitors in this series was low. These compounds were typically more active toward JNK1 with a few-fold selectivity over JNK2 (Table 1) and JNK3 (the activity against JNK3 was only determined for three selected compounds; the IC_{50} values for **8c**, **8d**, and **12** were 0.060 ± 0.003, 0.037 ± 0.004, and 0.12 ± 0.02 μM, respectively). Inhibitors were tested in in vitro JNK1 and JNK2 enzymatic inhibition assays, and those with IC_{50} less than 1 μM were also tested in a cellular assay measuring c-Jun phosphorylation inhibition in HepG2 cells.[16] The JNK1 inhibition data are used in the SAR analysis in this report. A simple methylamide, **8a**, gave an IC_{50} of 1.2 μM (calculated K_i = 0.4 μM[16]) in the JNK1 enzymatic assay. This potency translates into an 8.8 kcal/mol binding free energy to the enzyme. This value is well above the calculated binding energy (−1.6 kcal/mol) for an "average" drug containing the same functional groups according to Andrews' algorithm,[22] suggesting that **8a** matches the JNK1 binding pocket quite well. In fact, the most potent known noncovalent ligands of this size exhibit an ∼11 kcal/mol binding free energy.[23] Since the existing functional groups in **8a** are efficiently utilized, the main SAR development strategy was to add more functional groups to the lead compound to achieve better potency. Thus, the addition of a phenyl group to the amide methyl group (**8b**) provided a 4-fold increase in enzymatic potency. In the HepG2 cellular assay, **8b** demonstrated an IC_{50} of 1.6 μM. The difference between enzymatic and cellular activities is probably due to the higher ATP concentration in cells. A focused library of arylmethylamine amides were then synthesized and screened. 2,5-Dimethoxy analogue (**3**) showed a further 4-fold increase in enzymatic and cellular potency. However, this compound was metabolically unstable because of rapid demethylation and further oxidation of the electron-rich phenyl ring. Installation of a methylsulfonyl group at the 4-position of the phenyl ring in **8b** further increased enzymatic potency although cellular activity remained similar (**8c**). However, the hydrophilic and electron-withdrawing sulfonyl group greatly increased the metabolic stability of the inhibitor. Compound **8c** showed $t_{1/2}$ > 60 min in mouse, rat, and human microsomes and demonstrated a 38.8% rat oral bioavailability with a half-life of 3.4 h (Table 2). Inhibitor **8d** represented one of the best compounds in this series with comparable enzymatic potency compared to **8c** and an improved cellular activity and PK profile (Table 2). Replacing the phenyl group in **8b** with a 3-pyridyl group (inhibitor **8e**) resulted in an 8-fold increase in

Table 1. SAR Summary

compd	JNK1 IC_{50} (μM)	JNK2 IC_{50} (μM)	HepG2 c-Jun IC_{50} (μM)
3	0.071 ± 0.014	0.12 ± 0.020	0.64
6	>10	ND[a]	ND[a]
8a	1.2	0.61	ND[a]
8b	0.27 ± 0.041	0.19 ± 0.050	1.1 ± 0.5
8c	0.019 ± 0.001	0.12 ± 0.020	0.53 ± 0.066
8d	0.012 ± 0.005	0.053 ± 0.012	0.11 ± 0.005
8e	0.026 ± 0.004	0.041 ± 0.004	1.2 ± 0.026
8f	0.004 ± 0.001	0.011 ± 0.003	>10
8g	6.4	>10	>10
12	0.024 ± 0.009	0.074 ± 0.022	0.48 ± 0.083
13	0.075 ± 0.017	0.068 ± 0.019	0.41 ± 0.15
15	1.5	4.4	ND[a]
17a	0.39 ± 0.02	ND[a]	5.8
17b	0.23 ± 0.11	ND[a]	2.5

[a] ND, not determined.

Table 2. Rat Microsomes Stability and Rat PK Profile (Oral Dose at 5 mg/kg in 10% DMSO and 90% PEG-400) of **8c**−**e** and **12**

compd	rat microsomes $t_{1/2}$ (min)	$t_{1/2}$ (h)	C_{max} (μg/mL)	AUC (μg·h/mL)	*F* (%)
8c	>60	3.4	1.02	6.32	38.8
8d	>60	2.2	1.32	4.00	54.7
8e	*a*	0.5	2.92	3.80	32.7
12	>60	5.1	1.78	15.4	124

[a] **8e** showed a $t_{1/2}$ of 5 min in mouse microsomes.

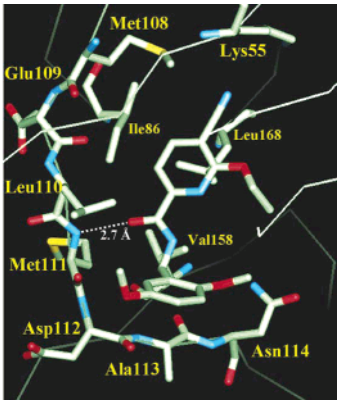

Figure 2. X-ray crystal structure of JNK1−**17b** complex (carbon is in white, oxygen is in red, nitrogen is in blue, and sulfur is in yellow).

enzymatic potency (almost equipotent to **8c**) but a comparable cellular activity. The reason that **8e** showed weaker cellular activity compared with **8c** is not clear because **8c** and **8e** demonstrated similar degree of protein binding and cell permeability (data not shown**)**. The electron-deficient pyridine ring in inhibitor **8e** was not as effective in preventing metabolic degradations. Inhibitor **8e** was cleared quickly and showed a $t_{1/2}$ of 0.5 h in rats, although it demonstrated a reasonable oral AUC and oral bioavailability (Table 2). Further derivatization of the pyridine ring in **8e** led to the discovery of **8f**, which showed the strongest potency in the enzymatic assay. Unfortunately, **8f** was inactive (IC_{50} > 10 μM) in the HepG2 c-Jun phosphorylation cellular assay. Replacing the 5-cyano group in **8c** with a chloro group led to inhibitor **12**. This compound was ~2-fold less potent than **8c** in enzymatic assay and comparable in cellular activity but provided a much-improved $t_{1/2}$, AUC, and a quantitative oral bioavailability. The close analogue 6-isopropyl ether **13** showed a decreased enzymatic inhibition potency and comparable cellular activity.[24]

Changes on the pyridine ring generally led to less active compounds. For example, the removal of the carbonyl group in **3** resulted in an inactive inhibitor (**6**). This is consistent with the observation that this carbonyl group makes a key hydrogen bond interaction with the hinge region of the enzyme (Figure 2). Methylation of the NH group in **8c** (inhibitor **8g**) caused a 300-fold loss of inhibitory activity against JNK1. Replacement of the ethoxy group in **8c** with a chloro group (inhibitor **15**) also led to a much weaker (70-fold less) inhibitor. Deletion of the 4-amino group resulted in a 5- to 20-fold loss of inhibitory activity (**17a** and **17b**).

The X-ray crystal structure of inhibitor **17b** in complex with JNK1 was solved at 3.0 Å resolution (Figure 2).[25] Inhibitor **17b** binds to the ATP binding site and makes several interactions with the hinge-binding region of the enzyme. The carbonyl group in **17b** is hydrogen-bonded to the Met111 NH group (2.7 Å).[13b] The pyridine ring interacts with the hydrophobic surface of the terminal methyl group of Met108 and the side chains of Ile86, Leu168, and Val158. The ethoxy group on the pyridine ring points to the ribose binding pocket, and the cyano group on the pyridine ring is in van der Waals contact with Lys55 and Met108. The phenyl ring in **17b** provides some hydrophobic interactions with Ile32 (not shown in Figure 2). The oxygen atom in the 2-methoxy group on the phenyl ring may stabilize the bioactive conformation via a long intramolecular hydrogen bond (3.2 Å) with the amide NH group. The 5-methoxy group on the phenyl ring is in van der Waals contact with Ala42 (not visible in Figure 2).

Table 3. Selectivity Profile of **12** against a Panel of 77 Kinases[a]

kinase	K_i (μM)	kinase	K_i (μM)	kinase	K_i (μM)
Abl	>0.7	ErbB4	>3.8	Nek2	>9.2
AKT1	>8.2	ERK2	3.4	P38δ	>6.8
AKT2	>8.4	FGFR	>4.7	P38γ	>7.5
AKT3	>9.5	FGFR3	>1.9	P70S6K	>6.7
AMPK	>9.8	Flt1	>0.44	PAK1	>9.7
Aurora1	>6.9	Flt3	>2.5	PAK4	>5.4
Aurora2	>6.7	Flt4	>7.0	PDK1	>3.8
Blk	>1.4	Fyn	>0.81	Pim1	>9.2
CaMK4	>8.5	Gsk3α	>8.9	Pim2	>1.4
CDC2	>8.9	GSK3β	>7.0	PKA	>7.5
CDC42	>9.5	IGFR	>1.0	PKCδ	>8.9
CDK2	>8.6	Ikkα	>3.8	PKCγ	>8.8
CDK5	>9.3	IKKβ	>3.1	PKCζ	>8.3
CHK1	>8.8	InsR	>5.2	Pkd2	5.2
CHK2	>9.5	Irak4	>9.9	Plk1	>8.9
Ck1δ	>7.8	ITK	>1.5	Plk3	>8.0
CK2	>5.8	JAK2	>1.4	Plk4	>4.3
cKit	>1.2	JAK3	>1.7	Rock1	>9.1
cMet	>2.8	JNK1	0.0038	Rock2	>7.5
CSF1R	>2.5	Kdr	>8.9	Rsk2	>7.4
CTAK	>6.7	Lck	>2.7	SGK	>9.4
Dyrk1A	>6.9	LIMK1	>9.5	Src	>1.9
EGFR	>1.8	Lyn	>1.6	TrkA	>2.5
EMK	>7.5	MAPKAPK	>8.4	TrkB	>4.5
EphA2	>8.0	MK3	>9.2	Tyk2	>1.9
ErbB2	>1.4	MST2	>8.8	Zipk	>1.4

[a] Values in Table 3 are calculated inhibition constants (K_i) from the Cheng−Prusoff equation, $K_i = IC_{50}/(1 + ([ATP]/K_m)$. See ref 16 for details.

The selectivity profiles of the more potent inhibitors against other kinases were studied using a kinase screening assay.[16] Under these assay conditions, excellent selectivity over a panel of 77 kinases was routinely achieved. For example, **12** showed no inhibitory activity toward other kinases in this panel at the highest concentration tested (Table 3) except ERK2 and Pkd2, but with a nearly a 1000-fold selectivity window.

Inhibitor **12** was also profiled in a panel of 74 receptors, ion channels, and enzymes and exhibited <30% inhibition to all of them at 10 μM. Inhibitors **8c** and **8e** were tested in a [^{3}H]dofetilide assay and showed weak hERG channel blockade activity (IC_{50} > 100 μM).

In conclusion, a series of potent and highly selective JNK inhibitors with good PK profiles were discovered. These high-quality JNK inhibitors could be valuable tools for evaluating the therapeutic relevance of inhibiting JNKs with small molecules. SAR results suggest that further studies of the amine moiety of the amides might lead to more potent inhibitors. The in vivo evaluation of some of the inhibitors in several disease animal models will be discussed in a separate report.

Acknowledgment. We thank Dr. David W. A. Beno for determining rat oral bioavailability and Dr. Yau Yi Lau for generating microsome stability data.

Supporting Information Available: Experimental procedures and spectral characterization of all final compounds. This material is available free of charge via the Internet at http://pubs.acs.org.

References

(1) Barr, R. K.; Bogoyevitch, M. A. The c-Jun N-terminal protein kinase family of mitogen-activated protein kinases (JNK MAPKs). *Int. J. Biochem. Cell Biol.* **2001**, *33*, 1047−1063
(2) Gupta, S.; Barrett, T.; Whitmarsh, A. J.; Cavanagh, J.; Sluss, H. K.; Derijard, B.; Davis, R. J. Selective interaction of JNK protein kinase isoforms with transcription factors. *EMBO J.* **1996**, *15*, 2760−2770.
(3) (a) Dong, C.; Yang, D. D.; Wysk, M.; Whitmarsh, A. J.; Davis, R. J.; Flavell, R. A. Defective T cell differentiation in the absence of Jnk1. *Science* **1998**, *282*, 2092−2095. (b) Yang, D. D.; Conze, D.; Whitmarsh, A. J.; Barrett, T.; Davis, R. J.; Rincon, M.; Flavell, R.

A. Differentiation of CD4+ T cells to Th1 cells requires MAP kinase JNK2. *Immunity* **1998**, *9*, 575−585. (c) Sabapathy, K.; Hu, Y.; Kallunki, T.; Schreiber, M.; David, J. P.; Jochum, W.; Wagner, E. F.; Karin, M. JNK2 is required for efficient T-cell activation and apoptosis but not for normal lymphocyte development. *Curr. Biol.* **1999**, *9*, 116−125.

(4) Yang, D. D.; Kuan, C. Y.; Whitmarsh, A. J.; Rincon, M.; Zheng, T. S.; Davis, R. J.; Rakic, P.; Flavell, R. A. Absence of excitotoxicity-induced apoptosis in the hippocampus of mice lacking the Jnk3 gene. *Nature* **1997**, *389*, 865−870.

(5) Wellen, K. E.; Hotamisligil, G. S. Inflammation, stress, and diabetes. *J. Clin. Invest.* **2005**, *115*, 1111−1119.

(6) (a) Kershaw, E. E.; Flier, J. S. Adipose tissue as an endocrine organ. *J. Clin. Endocrinol. Metab*. **2004**, *89*, 2548−2556. (b) Lazar, M. A. How obesity causes diabetes: not a tall tale. *Science* **2005**, *307*, 373−375.

(7) (a) Shin, E. A.; Kim, K. H.; Han, S. I.; Ha, K. S.; Kim, J. H.; Kang, K. I.; Kim, H. D.; Kang, H. S. Arachidonic acid induces the activation of the stress-activated protein kinase, membrane ruffling and H_2O_2 production via a small GTPase Rac1. *FEBS Lett.***1999**, *452*, 355−359. (b) Rizzo, M. T.; Leaver, A. H.; Yu, W. M.; Kovacs, R. J. Arachidonic acid induces mobilization of calcium stores and c-Jun gene expression: evidence that intracellular calcium release is associated with c-Jun activation. *Prostaglandins, Leukotrienes Essent. Fatty Acids*, **1999**, *60*, 187−198. (c) Kyriakis, J. M.; Avruch, J. Sounding the alarm: protein kinase cascades activated by stress and inflammation. *J. Biol. Chem.* **1996**, *271*, 24313−24316.

(8) Aguirre, V.; Uchida, T.; Yenush, L.; Davis, R. J.; White, M. F. The c-Jun NH_2-terminal kinase promotes insulin resistance during association with insulin receptor substrate-1 and phosphorylation of Ser^{307}. *J. Biol. Chem*. **2000**, *275*, 9047−9054.

(9) Aguirre, V.; Werner, E. D.; Giraud, J.; Lee, Y.; Shoelson, S. E.; White, M. F. Phosphorylation of Ser^{307} in insulin receptor substrate-1 blocks interactions with the insulin receptor and inhibits insulin action. *J. Biol. Chem*. **2002**, *277*, 1531−1537.

(10) Hirosumi, J.; Tuncman, G.; Chang, L.; Görgün, C. Z.; Uysal, K. T.; Maeda, K.; Karin, M.; Hotamisligil, G. S. A central role for JNK in obesity and insulin resistance. *Nature* **2002**, *420*, 333−336.

(11) Kaneto, H.; Nakatani, Y.; Miyatsuka, T.; Kawamori, D.; Matsuoka, T.; Matsuhisa, M.; Kajimoto, Y.; Ichijo, H.; Yamasaki, Y.; Hori, M. Possible novel therapy for diabetes with cell-permeable JNK-inhibitory peptide. *Nat. Med*. **2004**, *10*, 1128−1132.

(12) Bennett, B.; Satoh, Y.; Lewis, A. J. JNK: a new therapeutic target for diabetes. *Curr. Opin. Pharmacol*. **2003**, *3*, 420−425.

(13) (a) Gaillard, P.; Jeanclaude-Etter, I.; Ardissone, V.; Arkinstall, S.; Cambet, Y.; Camps, M.; Chabert, C.; Church, D.; Cirillo, R.; Gretener, D.; Halazy, S.; Nichols, A.; Szyndralewiez, C.; Vitte, P. A.; Gotteland, J. P. Design and synthesis of the first generation of novel potent, selective, and in vivo active (benzothiazol-2-yl)-acetonitrile inhibitors of the c-Jun N-terminal kinase. *J Med. Chem*. **2005**, *48*, 4596−4607. (b) Stocks, M. J.; Barber, S.; Ford, R.; Leroux, F.; St-Gallay, S.; Teague, S.; Xue, Y. Structure-driven HtL: design and synthesis of novel aminoindazole inhibitors of c-Jun N-terminal kinase activity. *Bioorg. Med. Chem. Lett*. **2005**, *15*, 3459−3462. (c) Ruckle, T.; Biamonte, M.; Grippi-Vallotton, T.; Arkinstall, S.; Cambet, Y.; Camps, M.; Chabert, C.; Church, D. J.; Halazy, S.; Jiang, X.; Martinou, I.; Nichols, A.; Sauer, W.; Gotteland, J. P. Design, synthesis, and biological activity of novel, potent, and selective (benzoylaminomethyl)thiophene sulfonamide inhibitors of c-Jun-N-terminal kinase. *J. Med. Chem*. **2004**, *47*, 6921−6934. (d) Manning, A. M.; Davis, R. J. Targeting JNK for therapeutic benefit: from junk to gold? *Nat. Rev. Drug Discovery* **2003**, *2*, 554−565.

(14) Middleton, W. J. U.S. Patent 2,790,806, 1957 (E. I. du Pont de Nemours and Co.). Metzger, R.; Oberdorfer, J.; Schwager, C.; Thielecke, W.; Boldt, P. Einstufensynthese von 2,4-bis(*sec*-alkylamino)-6-halogen-3-pyridincarbonitrilen (Synthesis of 2,4-bis(*sec*-alkylamino)-6-halogen-3-pyridincarbonitriles). *Liebigs Ann. Chem*. **1980**, 946−953.

(15) Junek, H.; Uray, G.; Kotzent, A. Isomere diamino-alkoxy-pyridincarbonitrile—ihre trennung und verwendung als kupplungskomponenten (Diaminoalkoxypyridincarbonitrile isomers—its separation and use as components). *Monatsh. Chem.* **1983**, *114*, 973−982.

(16) Szczepankiewicz, B. G.; Kosogof, C.; Nelson, L. T. J.; Liu, G.; Liu, B.; Zhao, H.; Serby, M. D.; Xin, Z.; Liu, M.; Gum, R. J.; Haasch, D. L.; Wang, S.; Johnson, E. J.; Lubben, T. H.; Stashko, M. A.; Olejniczak, E. T.; Sun, C.; Dorwin, S. A.; Haskins, K.; Abad-Zapatero, C.; Fry, E. H.; Hutchins, C. W.; Rondinone, C.; Trevillyan, J. M. Aminopyridine-based JNK inhibitors with cellular activity and minimal cross-kinase activity. *J. Med. Chem*. **2006**, *49*, 3563−3580. ATF-2 was the phosphorylation substrate, and 5 μM ATP was used in the JNK enzymatic assay. HepG2 human hepatoma cells were used in the cellular assay.

(17) Mittelbach, M.; Junek, H. Syntheses with nitriles. LXXIV. 3-Amino-4,4-dicyano-3-butenoate, a synthetically useful dimer from malononitrile and cyanoacetate. *Liebigs Ann. Chem*. **1986**, *3*, 533−544.

(18) Kingsbury, W. D.; Pendrak, I.; Leber, J. D.; Boehm, J. C.; Mallet, B.; Sarau, H. M.; Foley, J. J.; Schmidt, D. B.; Daines, R. A. Synthesis of structural analogues of leukotriene B4 and their receptor binding activity. *J. Med. Chem*. **1993**, *36*, 3308−3320.

(19) Fanta, P. E.; Stein, R. A. The condensation of sodium nitromalonaldehyde with cyanoacetamide. *J. Am. Chem. Soc*. **1955**, *77*, 1045−1046.

(20) Sakamoto, M.; Sano, T.; Fujita, S.; Ando, M.; Yamaguchi, K.; Mino, T.; Fujita, T. Regioselective photocycloaddition of pyridine derivatives to electron-rich alkenes. *J. Org. Chem*. **2003**, *68*, 1447−1450.

(21) Kosaku, H.; Kitade, Y.; Senda, S.; Halat, M. J.; Watanabe, K. A.; Fox, J. J. Pyrimidines. 17. Novel pyrimidine to pyridine transformation reaction. One-step synthesis of pyrido[2,3-*d*]pyrimidines. *J. Org. Chem*. **1981**, *46*, 846−851.

(22) Andrews, P. R.; Craik, D. J.; Martin, J. L. Functional group contributions to drug−receptor interactions. *J. Med. Chem*. **1984**, *27*, 1648−1657.

(23) Kuntz, I. D.; Chen, K.; Sharp, K. A.; Kollman, P. A. The maximal affinity of ligands. *Proc. Natl. Acad. Sci. U.S.A.* **1999**, *96*, 9997−10002. An exception is biotin, which binds to avidin with a binding energy of ∼19 kcal/mol.

(24) This modification provides a 2-fold increase in enzymatic potency for some analogues with different substitution patterns in the phenyl ring.

(25) The refined crystallographic coordinates have been deposited in the Protein Data Bank (www.rcsb.org) with entry code 2H96. For experimental details, see ref 16.

JM060465L